

See discussions, stats, and author profiles for this publication at: <https://www.researchgate.net/publication/231648081>

Interfacial Electronic Structure of the Dipolar Vanadyl Naphthalocyanine on Au(111): “Push-Back” vs Dipolar Effects

ARTICLE in THE JOURNAL OF PHYSICAL CHEMISTRY C · OCTOBER 2011

Impact Factor: 4.77 · DOI: 10.1021/jp204720a

CITATIONS

22

READS

44

8 AUTHORS, INCLUDING:



Aleksandrs Terentjevs
Italian National Research Council

20 PUBLICATIONS 160 CITATIONS

[SEE PROFILE](#)



Leah L Kelly
The University of Arizona

9 PUBLICATIONS 36 CITATIONS

[SEE PROFILE](#)



Eduardo Fabiano
Italian National Research Council

74 PUBLICATIONS 1,220 CITATIONS

[SEE PROFILE](#)



Fabio Della Sala
Italian National Research Council

182 PUBLICATIONS 5,057 CITATIONS

[SEE PROFILE](#)

Interfacial Electronic Structure of the Dipolar Vanadyl Naphthalocyanine on Au(111): “Push-Back” vs Dipolar Effects

Aleksandrs Terentjevs,[†] Mary P. Steele,[‡] Michael L. Blumenfeld,[‡] Nahid Ilyas,[‡] Leah L. Kelly,[‡] Eduardo Fabiano,[†] Oliver L.A. Monti,^{‡,*} and Fabio Della Sala^{*,†,§}

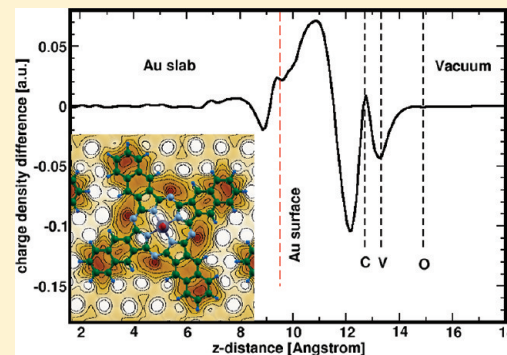
[†]National Nanotechnology Laboratory (NNL), Istituto Nanoscienze-CNR, Via per Arnesano 16, I-73100 Lecce, Italy

[‡]Department of Chemistry and Biochemistry, The University of Arizona, 1306 East University Boulevard, Tucson, Arizona 85721, United States

[§]Center for Biomolecular Nanotechnologies@UNILE, Istituto Italiano di Tecnologia (IIT), Via Barsanti, I-73010 Arnesano (LE), Italy

 Supporting Information

ABSTRACT: We investigate the interfacial electronic structure of the dipolar organic semiconductor vanadyl naphthalocyanine on Au(111) in a combined computational and experimental approach to understand the role of the permanent molecular dipole moment on energy-level alignment at this interface. First-principles Density Functional Theory (DFT) calculations on such large systems are challenging, due to the large computational cost and the need to accurately consider dispersion interactions. Our DFT results with dispersion correction show a molecular deformation upon adsorption but no strong chemical bond formation. Ultraviolet photoelectron spectroscopy measurements show a considerable workfunction change of $-0.73(2)$ eV upon growth of the first monolayer, which is well reproduced by the DFT calculations. This shift originates from a large electron density “push-back” effect at the gold surface, whereas the large out-of-plane vanadyl dipole moment plays only a minor role.



I. INTRODUCTION

Recent advances in organic semiconductor-based electronics have shown convincingly the need for a precise understanding of their interfacial electronic structure.^{1–5} It is by now widely accepted that the vacuum level at the organic/electrode interface may not align because of the presence of a sizable interfacial dipole. Different interpretations offered for the origin of this interface dipole include partial charge transfer into an induced density-of-states (DOS), integer charge-transfer, and purely quantum mechanical exchange effects.^{6–8} Such interfacial interactions are strongly dependent on the precise atomistic details of the surface and the adsorbed organic molecule, and many different chemical and physical effects can act simultaneously. Recently, significant progress has been achieved in distinguishing the different contributions, in part due to the application/development of novel computational and theoretical approaches.^{9–22}

Considerable effort has been expended to control the interfacial electronic structure.^{5,7,20,23} A microelectrostatic picture of interfaces was first developed by Mott and Littleton for transport in ionic salts^{23,24} and suggests that both vacuum-level and molecular electronic structure may be selectively influenced by the presence of molecular dipole moments. Consequently, a number of research groups have investigated the effects of a permanent dipole moment on the vacuum-level alignment at the

organic/metal interface from both an experimental and a theoretical point of view, with particular emphasis on chemisorbed self-assembled monolayers (SAMs).^{19,20,22,25–27} Alternatively, a permanent out-of-plane dipole may be built into a flat macrocyclic organic semiconductor.^{28–33} Detailed investigations of the interfacial electronic structure of thin films of dipolar phthalocyanines (Pc and Nc, respectively) on highly oriented pyrolytic graphite (HOPG) showed interfaces characterized by weak interactions between the semiconductor and surface due to the low HOPG DOS near the Fermi energy E_F . As a result, vacuum-level shifts and changes to the molecular electronic structure are dominated by intermolecular dipole–dipole coupling and image-charge effects.^{28–31} The applicability of this simple microelectrostatic perspective to metal substrates, with a high DOS near E_F as well as Shockley and Tamm surface states, can be expected to be modified by strong interfacial interactions which may alter the electronic structure substantially. Previous reports on different metal Pc's on metal substrates have in fact shown both strong and weak chemisorption and/or bonding/back-bonding interactions.^{34–40} However, these metal Pc's had at most a small intrinsic molecular dipole, and thus the

Received: May 21, 2011

Revised: September 16, 2011

Published: September 18, 2011

interplay of electrostatic effects with other interfacial interactions needs to be clarified to assess the extent to which interfacial electronic structure can be controlled by simple electrostatic considerations.

As a first step toward answering this question, we present here a combined computational and experimental study of the interfacial electronic structure of 1 monolayer (ML) of dipolar vanadyl naphthalocyanine (VONc) on Au(111). For this purpose, we have undertaken first-principles Density Functional Theory (DFT) calculations of the whole interface as well as photoelectron spectroscopy measurements. Crucially, few accurate investigations for Pc and none for Nc on metal surfaces have been reported in the literature; the majority of studies focuses on the smaller Pc's,^{36,38,39,41–45} without an accurate treatment of dispersion interactions, since such full DFT calculations are computationally challenging and very expensive. In this work, we describe the VONc/Au(111) interface considering full geometry optimizations in different adsorption sites and including a proper description of the dispersion interaction, essential for a correct treatment of this type of interface. We demonstrate that significant electronic charge reorganization occurs at the interface, dominating simple dipolar electrostatic effects.

II. MATERIALS AND METHODS

II.A. Experimental Section. The polished Au(111) crystal was purchased from Princeton Scientific (99.999% purity) and repeatedly sputtered (1.2 keV, 25 μA, room temperature) and annealed (550 °C, 1 h) prior to deposition. The presence of a clean, ordered $22 \times (\sqrt{3})$ surface was established by X-ray photoelectron spectroscopy, low-energy electron diffraction, the appearance of the sharp Tamm and strongly dispersive Shockley states (effective mass $m_{\text{eff}} = 0.27(1)$) in angle-resolved ultraviolet photoelectron spectroscopy (UPS), and a workfunction of 5.50(1) eV.^{46,47} Although coverages from 1 to 60 Å were investigated, we focus here on a film with 4 Å VONc (1 monolayer equivalent, 1 MLE, turning into 1 ML after annealing the film) for the sake of clarity.

VONc was purchased from Sigma-Aldrich and used without further purification. Prior to evaporation, the home-built Knudsen cell was repeatedly and slowly ramped to 470 °C for sample degassing while avoiding prolonged exposure to excessive cell temperatures that would risk thermal decomposition of VONc. Sample deposition occurred at 0.4 Å/min in a custom-built deposition chamber, with a base pressure of 1×10^{-9} Torr. Film thicknesses were determined using a quartz crystal microbalance and calibrated against the known thicknesses of VONc on HOPG.^{28,29}

The sample was introduced into the photoelectron spectrometer (VG Escalab MK II, base pressure 5×10^{-10} Torr) equipped with an integrated sample heater. All UPS spectra were referenced to the Fermi energy E_F and collected at room temperature using a He(I) lamp (Specs UVS 10/35, 30° angle of incidence from normal). Full spectra were recorded with a takeoff angle of 0° with respect to normal, ±12.5° acceptance angle, -5 V sample bias, and 5 eV pass energy. In the Fermi/highest occupied molecular orbital (HOMO) region, angular acceptance was restricted to ±1.5°. The VONc HOMO bands show no dispersion, indicative of localization in the surface plane. For a detailed analysis of the HOMO band, the spectra were background subtracted with an empirical combination of a constant offset and an exponential decay to take the proximity

of the Au d-bands into account. While the general conclusions reported here are unaffected by the precise choice of background, the chosen combination resulted in the least correlation between fitting parameters of the observed spectral features in the HOMO region. The vacuum level was measured from the baseline intercept with the spectral slope at the inflection point in the low kinetic energy region (secondary electron cutoff, SECO). From deconvolution of the Au Fermi edge, a spectral resolution of 89(8) meV was determined.

II.B. Computational Methods. Isolated Molecule. We performed DFT calculations for an isolated VONc molecule with the TURBOMOLE program⁴⁸ using the Perdew–Burke–Ernzerhof (PBE) exchange-correlation functional.⁴⁹ We used the def2-TZVPD basis set,^{50,51} which was recently proposed for an accurate description of polarizability.⁵¹

Note that the use of a local or semilocal (e.g., PBE) exchange-correlation functional yields, for the VONc molecule, a highest occupied molecular orbital (HOMO) occupied by only one electron and with an atomic-like V character.^{52,53} This feature is not observed in photoemission experiments on VOPc which instead suggest that the orbital involved in the first ionization process is a doubly occupied π -orbital extended over the whole macrocycle.⁵⁴ A correct description of the energy-level ordering can be obtained using, e.g., hybrid functionals which include a fraction of exact exchange (see Figure S2 in the Supporting Information). We note that similar descriptions have also been considered for other paramagnetic metal-phthalocyanines with one unpaired electron.^{55–61} The present computational study, which is mainly based on plane-wave calculations with periodic boundary conditions, is not affordable using methods beyond PBE, but we expect that the exact molecular orbital level ordering plays a negligible role for the quantities of interest in this work. For these reasons, the PBE functional was used throughout. Furthermore, we note that the presented theoretical calculations aim to model workfunction modifications and not the photoemission spectroscopy, which will require to include many-electron effects beyond DFT.

Periodic Monolayer and Interface. DFT calculations for the VONc monolayer on the Au(111) surface were performed using the plane-wave Quantum Espresso software package,⁶² employing PBE ultrasoft pseudopotentials. For all calculations, we used an energy (density) cutoff of 30 (300) Ry, in agreement with previous calculations for vanadium-containing materials (see, e.g., refs 63 and 64). Higher cutoffs led to unaffordable computational costs given the size of the system under investigation. The gold surface was modeled by a five-layer thick slab with a $(6 \times 4\sqrt{3})$ surface periodicity. We used a cell of 17 Å in the vertical direction and a dipole correction scheme.⁶⁵ The simulation cell included 322 atoms and 3.3 million G-vectors. The calculations were performed at the Γ point only. Higher k-point sampling leads to an unaffordable computational cost. The errors introduced by the Γ point approximation are expected to be smaller than the accuracy required for the discussion of results and comparison with experiments. A Gaussian smearing of 0.02 Ry was used to enhance convergence of the VONc/Au(111) and kept fixed for all other calculations. The threshold for energy convergence was set at 10^{-6} Ry.

For geometry optimizations, we relaxed all degrees of freedom but the bottom three gold layers, which were fixed to the bulk optimized lattice constant (4.137 Å, see next subsection regarding dispersion correction), in good agreement with the experimental value of 4.08 Å.⁶⁶

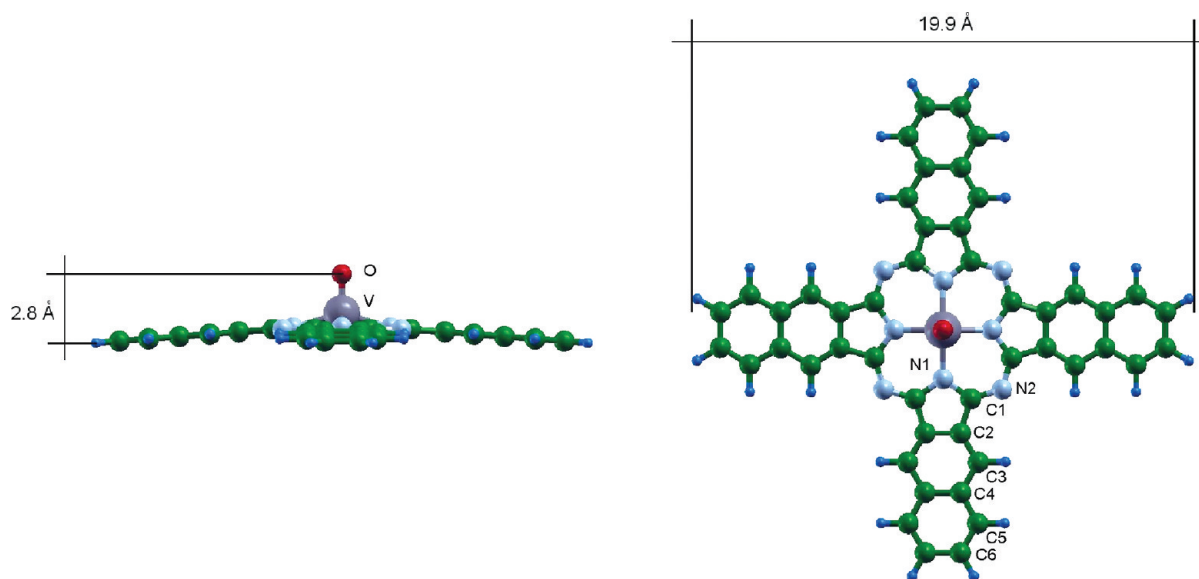


Figure 1. Optimized VONc molecular geometry in the free monolayer. The symmetry-inequivalent atoms are indicated.

The adiabatic adsorption energy E_{ads} was calculated from $E_{\text{ads}} = -(E^{\text{TOT}} - E^{\text{SLAB}} - E^{\text{SAM}})$, where E^{TOT} , E^{SLAB} , and E^{SAM} are the energies of the total system, the gold slab, and the periodic molecular VONc monolayer, respectively, both of them fully relaxed at their equilibrium conformation.

The workfunction shift $\Delta\Phi$ can be decomposed into the vacuum level shift of the isolated, relaxed molecular layer (ΔV_{vac}) and a bond-dipole (BD) component^{19,20,22}

$$\text{BD} = \int_0^L z \Delta\rho(z) dz \quad (1)$$

where the z -axis is perpendicular to the gold surface; L is the length of the unit cell in the z -direction (i.e., perpendicular to the substrate); and the *plane averaged charge-density difference* $\Delta\rho(z)$ is

$$\Delta\rho(z) = \int dx dy \Delta\rho(x, y, z) \quad (2)$$

The *charge-density difference* is given by

$$\Delta\rho(x, y, z) = \rho^{\text{TOT}}(x, y, z) - \rho^{\text{SLAB}}(x, y, z) - \rho^{\text{SAM}}(x, y, z) \quad (3)$$

that is, the density difference between densities for the total system, gold slab, and VONc monolayer.

We also considered the corresponding *electrostatic potential difference*

$$\Delta V(x, y, z) = V^{\text{TOT}}(x, y, z) - V^{\text{SLAB}}(x, y, z) - V^{\text{SAM}}(x, y, z) \quad (4)$$

Dispersion Correction. To understand the interfacial electronic structure, the precise determination of the VONc adsorption geometry on Au(111) is of fundamental importance. It is well-known that, in the absence of pinning,⁶⁷ small modifications of the metal–molecule distance can lead to significant changes in the electronic properties and, as a consequence, in a workfunction shift.^{68–72} A key issue in the DFT geometry optimization of metal–molecule interfaces is the proper treatment of the

exchange-correlation effects. Due to the very large size of the molecule under investigation, methods beyond the local density approximation (LDA) or the generalized gradient approximation (GGA) are out of reach. These functionals lack, however, the correct treatment of dispersion forces. Different theoretical investigations show that LDA leads to excessive binding energies,^{73–75} whereas GGA generally strongly underestimates binding energies.^{70,73–76}

To include dispersion interactions in DFT in an efficient way, we used in all our calculations the empirical correction scheme of Grimme,⁷⁷ recently implemented in the Quantum-Espresso package.⁷⁸ However, the empirical dispersion correction has been so far mostly applied to molecular systems only, and no well-defined C_6 parameter is available for bulk gold. Therefore, we investigated different possibilities: Using the C_6 parameter derived from atomic calculations (see ref 70), a somewhat excessive adsorption energy (~10 eV) was found for VONc/Au(111); similar results were also found for pentacene on Au(111).⁷⁰ In addition, we found that this parameter significantly underestimates the gold lattice constant, making it inadequate for determining an accurate interfacial geometry. In a second attempt, we used the C_6 parameter obtained by Tonigold et al.,⁷⁶ yielding an accurate bulk gold lattice constant (4.137 Å) and even improving on the result without dispersion correction.⁷⁹ In addition, the adsorption energy of the VONc/Au(111) interface is reduced by about a factor of 2 (see Section III.C) and, as discussed in refs 70 and 76, in the correct energy range. A similar value for the C_6 parameter has already been used in ref 80. We used this C_6 parameter for all geometry optimizations of periodic structures presented in this work, while the default parameters from ref 77 were used for all other atoms. The dispersion-corrected PBE method is defined hereafter as PBE+D.

III. RESULTS

III.A. Structural and Electronic Properties of the Isolated Monolayer. The PBE+D optimized VONc geometry of the periodic monolayer in the absence of the Au surface is shown in Figure 1. The *calculated* “monolayer” corresponds in fact to a true

Table 1. Computed Energetic and Structural Data for the Isolated VONc SAM and the Atop and Bridge Interface^a

system	V–O (Å)	ΔzC (Å)	ΔV_{vac} (eV)	μ (D)	α_{zz} (a.u.)	E_{ads} (eV)	$\langle \Delta z \rangle$ (Å)	Au–V (Å)	BD (eV)	$\Delta \Phi$ (eV)
free VONc	1.59	0.48	+0.25	2.67	306	-	-	-	-	-
atop	1.59	0.24	+0.25	2.48	302	5.40	3.19	3.89	-0.73	-0.48
bridge	1.59	0.10	+0.22	2.11	301	5.49	3.18	3.79	-0.72	-0.50

^a The first five columns are related to the properties of the VONc SAM, in different geometrical conformation (isolated or interacting with the substrate), and indicate (from left to right): the distance between vanadium and oxygen atom (V–O), the maximum distance between the z coordinate of the carbon atoms of the VONc molecule (ΔzC); the vacuum level shift ΔV_{vac} resulting purely from electrostatic potential of the free layer of molecular dipoles; and the intrinsic dipole moment (μ) and polarizability (α_{zz}) of the isolated VONc molecule from PBE/def2-TZVPD calculations. The last five columns are related to the properties of the interface (atop or bridge) and indicate (from left to right): the adiabatic total adsorption energy of VONc on the Au surface (E_{ads}), the averaged distance between the VONc carbon atoms and the Au surface atoms ($\langle \Delta z \rangle$); the distance between the vanadium atom of VONc and Au surface atoms (Au–V); the bond dipole (BD); and the total workfunction shift ($\Delta \Phi$).

0.75 ML coverage, ensuring that van der Waals type intermolecular forces are negligible (see Section III.C for more detail). The naphtha-groups are slightly bent, in agreement with the shuttlecock geometry of dipolar MPc and MNc:^{28,31} the maximum distance in the out-of-plane coordinate of the carbon atom is 0.48 Å, and the V–O bond length in VONc is 1.59 Å (see Table 1), in excellent agreement with experimental results for VOPc.⁸¹ The total height of the molecule is 2.8 Å. The V–O group creates a permanent large dipole moment perpendicular to the plane of the molecule, calculated to be 2.38 D in the free monolayer. A corresponding vacuum level shift of about +0.25 eV (see Table 1) due to the array of ordered dipoles is calculated in the isolated monolayer. This value is in agreement with experiments of VONc on weakly interacting HOPG, where a workfunction increase of +0.21(1) eV was found at 1 ML and of about +0.19 eV at 0.75 ML.²⁹ Note that the present comparison is necessarily approximate also due to the neglect in our calculations of the HOPG substrate effects, which, although small, can slightly decrease the experimental work-function shift.

Note that the aforementioned value of the dipole moment takes into account depolarization effects^{16,82} due to surrounding VONc molecules in the full monolayer. Calculations performed for the *isolated* VONc molecule, i.e., without periodic boundary conditions, with the same geometry and the same DFT functionals yielded a larger value of the dipole (2.67 D). This is in excellent agreement with a previous experimental estimate for isolated VONc on HOPG of 2.7(4) D.²⁹ The computed static polarizability (zz component, α_{zz} in the following) is also reported in Table 1, due to polarization of the V–O dipole as well as out-of-plane polarization of the π -electron system. Note that the experimental estimate for α_{zz} represents an *effective* polarizability which also includes the effect of the HOPG substrate,²⁹ thus somewhat larger than the value reported in Table 1.

III.B. UPS Spectra of the VONc/Au(111) Interface. Figure 2 shows a UPS survey spectrum of the clean $22 \times (\sqrt{3})$ surface in comparison with that of an annealed 1 ML VONc/Au(111). Upon adsorption of 1 MLE VONc, the Shockley and Tamm states are completely quenched, indicative of strong interaction between the VONc molecules and the surface. The HOMO band of VONc shows no marked dispersion from $k_{||} = 0$ to 1.6 \AA^{-1} , but instead a strong angular intensity dependence indicating a well-defined adsorption geometry.⁸³ Thus, a considerably improved signal-to-noise ratio may be obtained at 1 ML in high-resolution scans of the Fermi region at a takeoff angle of 25° (angle of maximum intensity) due to photoemission selection rules and molecular orientation, without causing any change of the

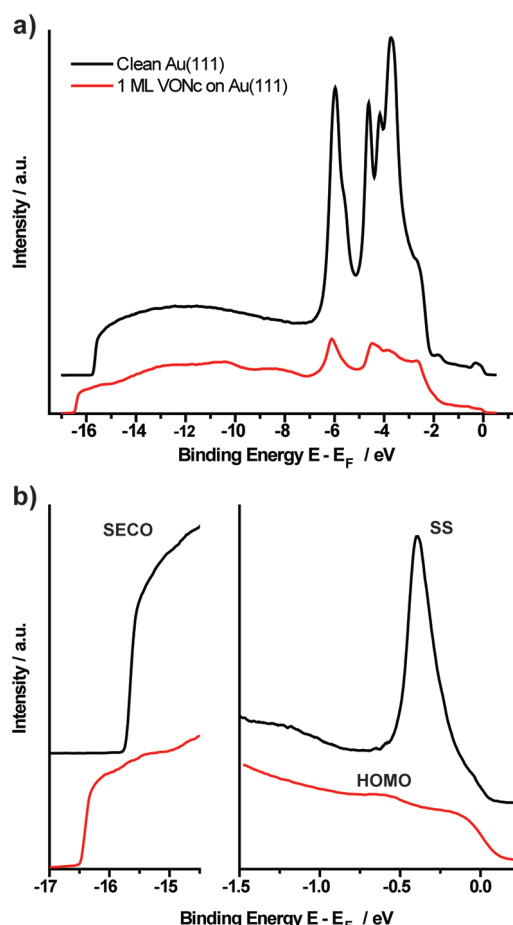


Figure 2. (a) Survey UP spectra of clean Au(111) $22 \times (\sqrt{3})$ (black) and annealed 1 ML VONc on Au(111) (red) at a 0° takeoff angle. The spectral intensities are to scale. (b) Left panel: Secondary-electron cutoff (SECO) region. Right panel: Close-up of the Fermi region, showing the occupied Au Shockley surface state (SS, part b) and the VONc HOMO.

observed band shape. A close-up spectrum of this region in the as-deposited film (Figure 3a) shows the presence of two features with comparable integrated intensity. Fitting with Voigt profiles yields a remarkably narrow feature (W) with a full-width-half-max (fwhm) of $\Gamma_W = 0.22(3)$ meV and a binding energy of $0.60(2)$ eV and a somewhat broader feature (M , $\Gamma_M = 0.27(5)$ meV) with binding energy $0.80(2)$ eV. Mild annealing at temperatures of 125°C for 1 h has a dramatic effect on the appearance of these spectra (Figure 3b), converting M quantitatively to W .

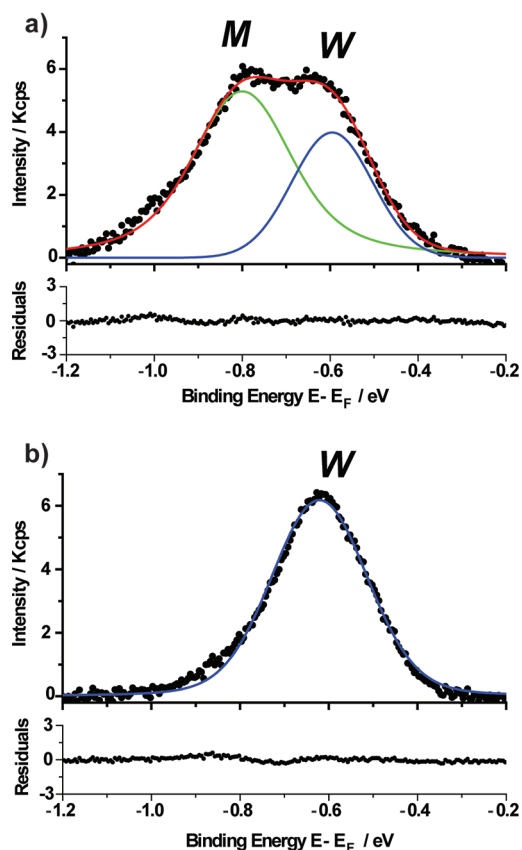


Figure 3. (a) Close-up background-subtracted UP spectrum, fit and residuals of unannealed 1 MLE VONc/Au(111) obtained at a takeoff angle of 25°. The HOMO feature could be fit with two Voigt peaks representing the wetting layer (*W*) and the multilayer structure (*M*). (b) Same as (a) but for the annealed film, showing only the *W* feature.

($\Gamma_W = 0.26(2)$ meV) at a binding energy of 0.62(1) eV. This conversion is also apparent in the increase of intensity of the *W* feature after annealing. In contrast to VONc/HOPG,²⁹ no conclusive evidence for vibronic progressions is found within the *W* band. At thicknesses above 1 MLE, annealing was no longer able to remove the *M* peak completely, allowing assignment of this feature to multilayer structures of VONc; its width is consistent with some structural disorder expected for a multilayer island phase. Conversely, the *W* feature constitutes therefore the “wetting layer” on the Au surface, with overall reduced disorder and hence relatively narrow fwhm at 1 MLE coverage. These results suggest that annealing affords an ordered 1 ML film of VONc.

For VONc/HOPG, several different molecular orientations were observed in the unannealed films, characterized as “O up”, “O down”, and “O paired”.^{28,29} The unannealed as-deposited spectra of VONc/Au(111) do not show clear evidence of such a distribution of orientations on the surface since an O-paired feature is missing for all surface treatments and coverages between 0 and >2 ML. Instead, the narrow wetting-layer peak contains likely only a single orientation, assigned as O up based on scanning tunneling microscopy and photoelectron diffraction studies for the related VOPc^{81,84} and as modeled here.

These conclusions are further supported by the appearance of a sharp, well-defined SECO upon annealing, as expected for the formation of an ordered, stable interface. Note that in contrast to

VONc/HOPG the workfunction drops from $\Phi = 5.50(1)$ eV on clean Au(111) $22 \times (\sqrt{3})$ to $\Phi = 4.77(2)$ eV, a net change of $\Delta\Phi = -0.73(2)$ eV. Prolonged annealing at much higher temperatures leads to a reemergence of the surface states and an increase in the workfunction, suggesting the formation of aggregate structures and bare Au patches on the surface.

III.C. Structural Properties of the VONc/Au(111) Interface.

On the basis of the combination of the present UPS spectra and the geometry reported for VOPc/Au(111),⁸¹ we adopt this flat-lying O-up geometry for all subsequent calculations. Note that the persistence of the $22 \times (\sqrt{3})$ reconstruction in the monolayer film cannot be excluded based on the UPS data despite quenching of the surface states, as suggested for both VOPc and CuPc.^{84,85} A full theoretical treatment of this effect is however beyond currently available computational capabilities because of the large size of the required unit cell. We therefore adopted an unreconstructed Au surface geometry and performed geometry optimization for two adsorption sites: *atop*, where the vanadyl group is exactly above a surface gold atom (Figure 4a), and *bridge*, where the vanadyl group is at an intermediate position between two surface gold atoms (Figure 4b). For both configurations, the orientation of the perpendicular naphthalo branches of the molecule are chosen along the [121] and [101] directions. These choices are justified by both experimental and computational work on the related MPC molecule class on Au(111): The adsorption orientations are in good agreement with STM results of the related DyPc and FePc on Au(111),^{86,87} while the adsorption sites correspond to the preferred sites determined for MPc/Au(111) in both computational and STM studies.^{45,86}

Note that the surface unit cell of VONc/Au(111) is not known. Likely, growth is *incommensurate* as already suggested for MPcs on various metal surfaces,^{34,35,71} such that a combined overlayer and substrate unit cell does not exist or includes instead a very large number of molecules. In consideration of these facts, the configurations reported in Figure 4 represent the smallest nonreconstructed orthorhombic unit cell with one molecule per cell. This unit cell provides also the highest possible molecular coverage while avoiding strong intermolecular repulsion caused by interactions between hydrogen atoms from different molecules. The associated coverage is approximately 0.75 ML, estimated from the ratio of molecular area to available surface area. In the present theoretical efforts, higher coverages can only be obtained with a prohibitively large unit cell (many times the size of the one chosen here) and containing multiple VONc's, leading to unaffordable computational cost. Even though this coverage is lower than the experimental 1 ML, it is sufficiently large to capture the relevant physics, as will be evident from the good agreement between experimental and computational results.

The computed PBE+D adsorption energy for VONc on the gold surface and the main geometrical parameters are presented in Table 1. We found an adsorption energy of about 5.5 eV and average metal–molecule distance $\langle \Delta z \rangle$ of about 3.2 Å. Although accurate experimental adsorption energies are currently not available for this system, Ziroff et al. demonstrated recently that adsorption energies on Au(111) and other noble metal (111) surfaces can be estimated from a simple model potential relating adsorption energy to the molecular area.⁸⁸ Adsorption energies of 1.5–2 eV were found for NTCDA and PTCDA,^{88,89} suggesting that the relevant value for VONc is expected to be around 4 eV given the much larger molecular size, in qualitative agreement with the calculated value. Moreover,

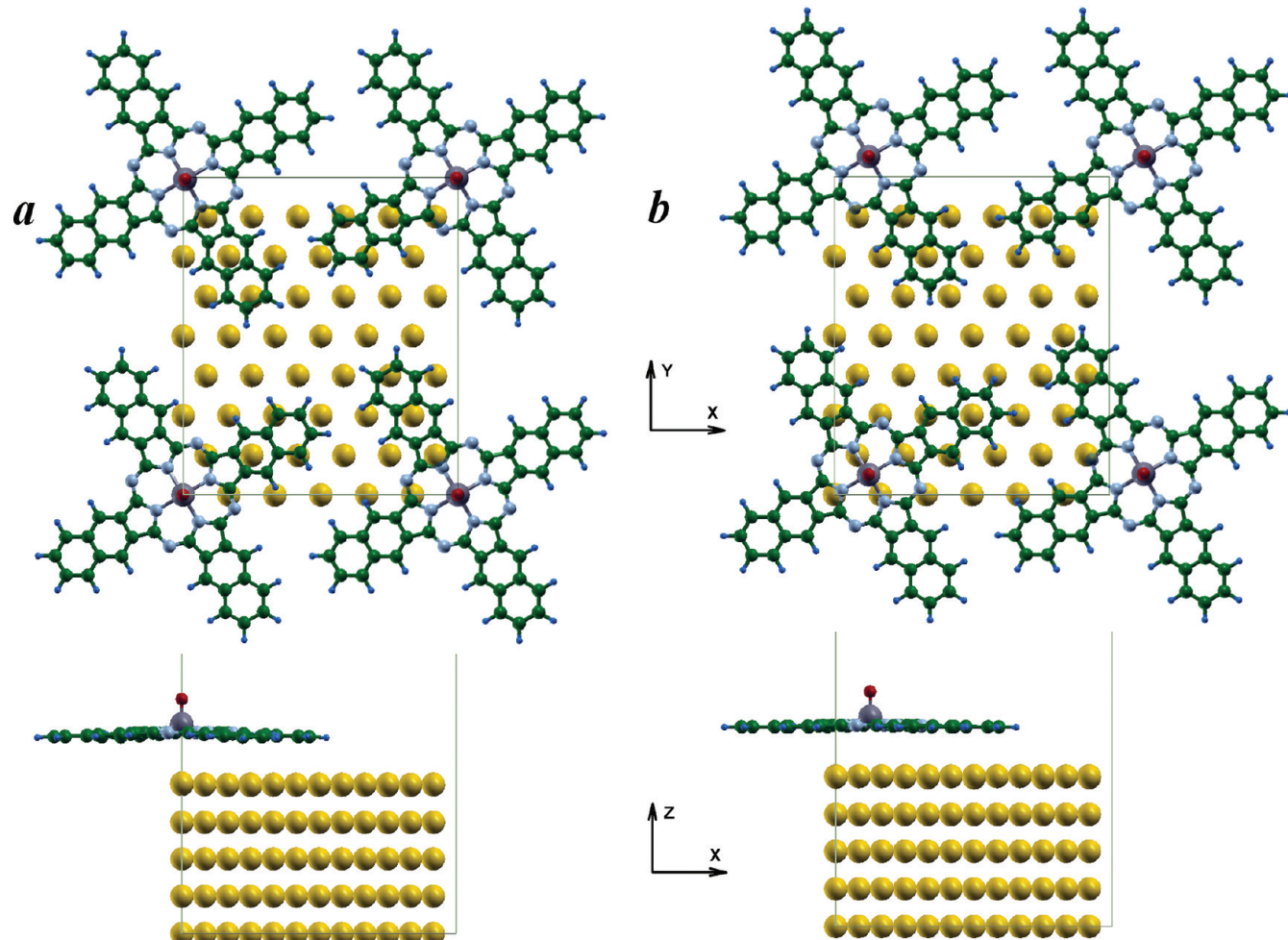


Figure 4. (a) Atop and (b) bridge unit cell for the VONc/Au(111) interfaces.

previous calculations of large organic molecules on Au(111) give adsorption metal–molecule distances of about 3 Å⁶⁸ in good agreement with our computed $\langle \Delta z \rangle$. We conclude therefore that the dispersion correction scheme with a C_6 parameter from ref 76 correctly describes the interfacial physics, even though an exact nonempirical treatment is out of reach for current state-of-the-art theoretical methods.

When comparing different adsorption geometries, the energy for adsorption at the bridge site is slightly lower than for the atop site, with an energy difference of about 0.1 eV. This is caused by the slightly shorter average distance between the Au surface and the VONc carbon atoms at the bridge site (0.01 Å). Such small energy differences are probably beyond the computational accuracy of the PBE+D method, so that no preferred adsorption site can be established with certainty. Note in addition that zero-point vibrational corrections, whose calculation is unaffordable for the present system, are also neglected.

Interestingly, we found that VONc flattens due to relaxation, thereby decreasing the largest vertical distance between atoms Δz_C from 0.48 to 0.24 Å in the atop and to 0.10 Å in the bridge geometry. This is in agreement with the recent photoelectron diffraction data of VOPc on Au(111).⁸¹ The larger flattening of VONc for the bridge site also makes the average distance between the Au surface and the VONc vanadium atom shorter by about 0.1 Å. Note that the vanadium oxygen bond length

remains the same for both sites. Interestingly, flattening of the molecule also reduces the intrinsic molecular dipole moment of the isolated molecule on the Au surface, decreasing to 2.48 D in the atop geometry and to 2.11 D in the bridge geometry, with a corresponding reduction of ΔV_{vac} of about 0.03 eV.

III.D. Electronic Properties of the VONc/Au(111) Interface. In this section, we will analyze in detail the results for the bridge site, which is predicted to be the ground state at the PBE+D level. Results for the atop configuration (not discussed hereafter) are very similar (see Table 1).

In Figure 5 (panel c), we report the DOS of the full metal–molecule interface projected onto different atom types and calculated at the Γ point. Panel (a) and (b) report the corresponding projected DOS (PDOS) of the isolated VONc monolayer and of the isolated gold slab, respectively. Note that for a more direct comparison with the full interface we considered the isolated systems in their final relaxed geometry of the interface. Moreover, the plot was obtained applying to all PDOSs the same Gaussian broadening, corresponding to the Gaussian smearing used in the quantum-mechanical calculations (see Computational Details). Therefore, the peaks in the PDOS of the free-standing monolayer (panel a) are artificially broadened (see figure S1 in the Supporting Information for a plot with lower broadening). The energies are relative to the Fermi level of each system. The PDOSs of the free-standing monolayer and of the

total system refer to the sum of the two spin channels (an analysis of the spin polarization is not relevant for the present discussion; see Figure S2 in the Supporting Information for the spin-resolved PDOS of the isolated monolayer). Comparing the PDOS of the full system (panel c) projected on the V, C, N, or gold atoms with the data in panels (a) and (b) shows that no significant modifications occur: beyond slight broadening for the C and N PDOS, orbital peaks shift less than 0.2 eV, showing that no strong chemical bonds are formed.

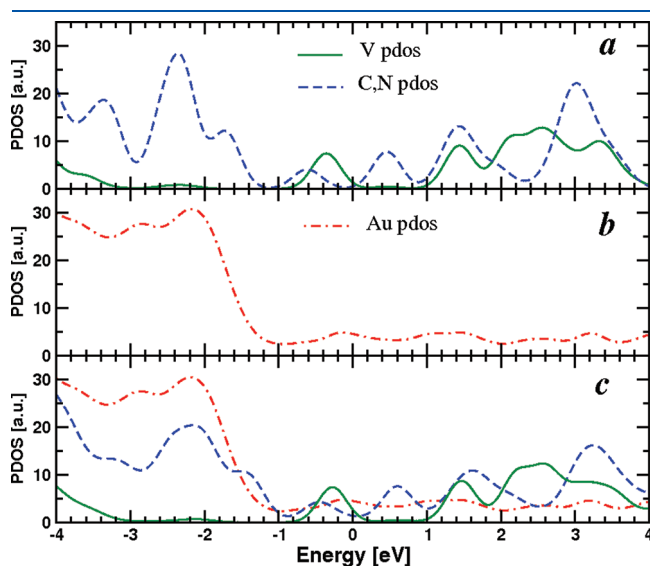


Figure 5. Projected density of states (PDOS) on V, C, N, and Au atoms for the isolated monolayer (a), isolated gold slab (b), and VONc/Au(111) interface (bridge configuration) (c). The PDOS on gold atoms is divided by a factor 20, and the PDOS on vanadium is multiplied by a factor of 4. The energy is relative to E_F for all atoms.

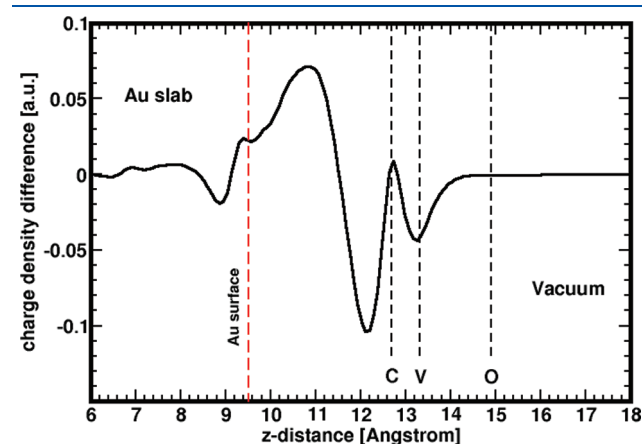


Figure 6. Computed plane-averaged charge density difference for bridge configuration. The dashed lines indicate the average positions for the C, V, and O atoms.

Table 2. Net Charges (au) from Population Analysis for Atoms Indicated in Figure 1 for the Isolated VONc SAM and the Bridge Configuration

atom	V	O	N ₁	N ₂	C ₁	C ₂	C ₃	C ₄	C ₅	C ₆
free VONc	0.32	-0.18	-0.23	-0.25	0.29	0.03	-0.11	0.05	-0.12	-0.13
bridge	0.31	-0.17	-0.21	-0.22	0.29	0.03	-0.09	0.05	-0.10	-0.10

Figure 6 shows the plane-averaged charge density difference (eq 2) and indicates a substantial charge reorganization at the interface, with a depletion of electron density near the molecule and a corresponding accumulation of charge near the metal surface. Integration of the charge density difference yields a molecule-to-metal charge-transfer of about 0.7 e. Interestingly, the charge originates mostly from the π -electron system and vanadium atom, while the O atom seems to be largely acting as a spectator.

The interfacial interaction and charge redistribution generate an adsorbate-induced dipole in the surface region pointing with the positive end toward vacuum, hence lowering the workfunction. This dipole, created by the variation of the plane-averaged charge density, is formally identical to a bond dipole and results in a workfunction shift of -0.72 eV. For the total workfunction shift $\Delta\Phi$, ΔV_{vac} from the suspended ML has to be added. Despite geometrical relaxation at the interface, ΔV_{vac} shows a negligible change upon adsorption to the Au surface (see Table 1), as it mainly originates from the VO dipole, mostly unaltered by adsorption. The total workfunction shift for bridge adsorption is thus about -0.50 eV. A very similar value (-0.51 eV) is computed considering the difference between the electrostatic potential and the Fermi energy in the vacuum region. The agreement with our UPS experiment (-0.73 eV) is remarkable considering that (i) the calculations are performed with a lower coverage (0.75 ML) than in the experiment and (ii) the metal–molecule distance plays a key role in the exact determination of the workfunction shift.⁷⁰

IV. DISCUSSION

The experimental $\Delta\Phi$ is $-0.73(2)$ eV, i.e., large and *in the opposite direction* of the corresponding change of $+0.21(1)$ eV for VONc/HOPG,^{28,29} where a simple microelectrostatic picture of oriented molecular dipoles was sufficient to rationalize the experimental finding. The theoretical analysis in Figure 6 predicts that a push-back effect⁸ is mainly responsible for this modification of the workfunction. The sizable change of the workfunction is indicative of the qualitatively different physics at the Au and HOPG interfaces; therefore, a model of the VONc/Au interface as a simple addition of an oriented dipolar layer to an inert surface as used for VONc/HOPG is not sufficient. VONc interacts with Au(111) with a strong wave function overlap and significant charge transfer toward the Au surface, but no specific chemical bonds are formed. Taken together, these effects lead to a strong interface dipole and a substantial decrease of the workfunction, dominating any anticipated effects from the permanent molecular dipole moment. While the presence of a molecular dipole moment can still be used to influence $\Delta\Phi$, explicit interfacial interactions dominate in the case of large, flat organic semiconductors.

Note that in contrast to MPC's^{45,90} there is no significant charge transfer from the V d-orbitals to the substrate. Table 2 reports the total atomic net charges from population analysis for the isolated VONc and the bridge configuration. The charge

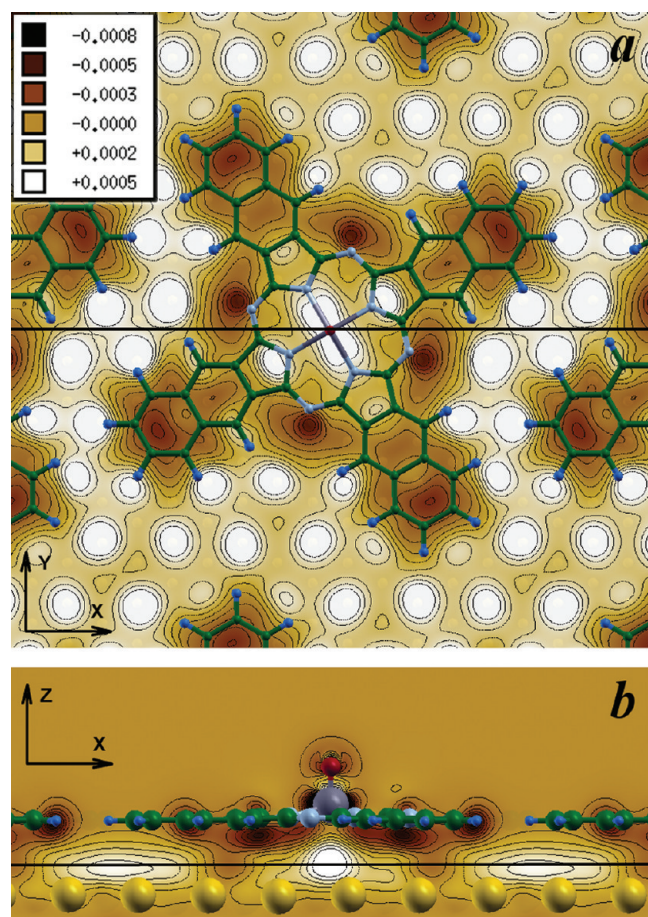


Figure 7. Charge difference map for bridge configuration in (a) the xy -plane at $z = 1.38 \text{ \AA}$ above the Au surface (see horizontal line in panel (b)) and (b) in the zx -plane containing the vanadyl group (see horizontal line in panel (a)).

difference on vanadium decreases by only 0.01e. This can be traced back to the quite large distance (3.8 Å, see Table 1) between the vanadium atom and the surface.

Even though the conventional analysis presented in Figure 6, generally used to understand the effect of SAMs on interfacial electronic structure,²⁰ captures the total workfunction shift, it is based on the density integrated across the whole xy plane, thus averaging over all in-plane effects. These can however be extremely important for a molecule as large as VONc in particular and likely for many other flat-lying organic semiconductors. Insight into the nature of the surface density modifications can be obtained by considering the charge difference map,⁵ calculated both in the xy -plane at $z = 1.4 \text{ \AA}$ above the Au surface (Figure 7a)—corresponding to the maximum positive peak in Figure 6—and in the zx -plane containing the vanadyl group (Figure 7b). Figure 7 shows that there are regions of large electron density increase (white) below the center of the molecule, below hydrogen atoms, and in the interstitial space between neighboring VONc molecules. At the same time, there are regions with a net electron density decrease (brown) in other regions of the molecule, below external nitrogen atoms (N2 in Figure 1), and below the naphthalo branches. At first sight, Figure 7 appears to show that the push-back effect is dominated by the molecular backbone repelling the electronic density

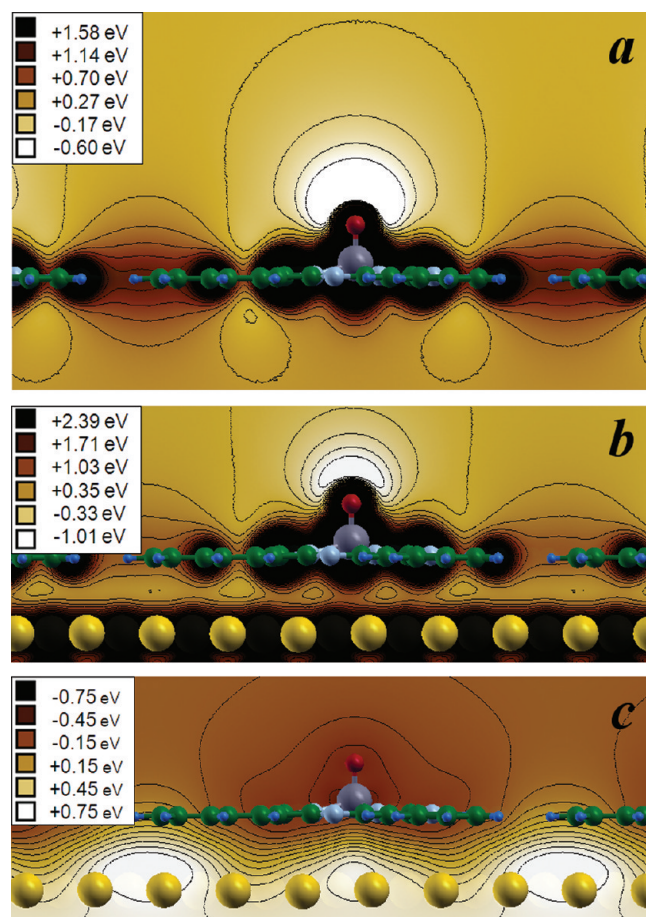


Figure 8. Electrostatic potential in the zy -plane containing the vanadyl group for the isolated monolayer (a) and the VONc/Au(111) interface (b). Panel (c) shows the electrostatic potential difference (see eq 4). The zero of the electrostatic potential is assumed to be far above the molecule.

toward the area between the molecules. However, careful inspection of Figure 7 reveals that the push-back effect is quite different at different points of the molecular backbone (e.g., near the external nitrogen N2); moreover, the density is *increased* in the center of the molecule, precluding a simple interpretation dominated by the molecular backbone.

The overall rationale of using dipolar molecules such as in SAMs or organic semiconductors with intrinsic molecular dipole moments is to influence energy level alignment and electronic structure at the interface. The presence of a layer of oriented molecules with sizable molecular dipole moment at an electron-rich surface such as Au(111) is thus expected to have a significant influence on the interfacial electronic structure. Figure 7b shows, however, that the induced electronic density below the vanadium atom is quite small and comparable in magnitude to the density induced between molecules as well as below hydrogen atoms. This is quite surprising considering the strong V–O dipole, expected to attract large electronic density in the interfacial space. This suggests the molecular dipole moment is not fully developed in the interfacial region. Indeed, even in the isolated monolayer, the electrostatic potential does not display the two-lobe structure of a classic electrostatic dipole, as can be seen in Figure 8a in a cut through the zx plane. While the negative lobe due to the oxygen charge is clearly visible above the molecule, the

positive charge of the vanadium atoms is screened below the molecule by the quadrupole moment of the π -electron system, and the corresponding positive lobe is missing. This screening by the Nc ring system destroys the notion that a dipolar MNc can be adequately represented as a point dipole and implies that previous electrostatic models may have to be reconsidered.^{28–31}

Importantly, when the molecular monolayer is connected to the gold substrate (Figure 8b), the profile of the electrostatic potential hardly changes. The electrostatic potential difference (see eq 4) is shown in Figure 8(c). This potential is slightly positive on the gold side of the interface and decreases above the surface to negative values. The overall appearance of this potential profile resembles that of an extended dipole, creating in effect the appearance of the bond-dipole as presented in Figure 6. Note that there is a significant potential “corrugation” along the molecular plane due to the local electrostatic effects.

V. CONCLUSIONS

In this combined experimental and theoretical study, we investigated the interfacial electronic structure of a monolayer of the dipolar organic semiconductor VONc on Au(111). Adsorption of 1 ML VONc on clean Au(111) results in a lowering of the workfunction by 0.73(2) eV, in good agreement with a state-of-the-art dispersion-corrected DFT calculation of this interface. The observed total workfunction change is *in the opposite direction* of the corresponding change when considering only the electrostatic component generated by the array of oriented VONc. The large bond–dipole component reflects negligible charge transfer and extensive push-back. The VO dipole moment does not show significant interaction with the metal substrate since it is substantially screened by the Nc ring itself.

■ ASSOCIATED CONTENT

5 Supporting Information. Projected density of states with smaller broadening and for the two spin channels. Energy levels of the isolated VONc molecule with different functionals. This material is available free of charge via the Internet at <http://pubs.acs.org>.

■ AUTHOR INFORMATION

Corresponding Author

*E-mail: monti@u.arizona.edu (O.L.A.M.); fabio.dellasala@unisalento.it (F.D.S.). Tel.: +1 520 626 1177 (O.L.A.M.); +39 0832 298202 (F.D.S.). Fax: +1 520 621 8407 (O.L.A.M.); +39 0832 298237 (F.D.S.).

■ ACKNOWLEDGMENT

This work was partially funded by the European Research Council (ERC) Starting Grant FP7, Project DEDOM, Grant Agreement No. 207441, and the National Science Foundation (CHE-0618477). M.P.S. was supported as part of the Center for Interface Science: Solar Electric Materials, an Energy Frontier Research Center funded by the U.S. Department of Energy, Office of Science, Office of Basic Energy Sciences under Award Number DE-SC0001084. M.L.B. also acknowledges a National Science Foundation Graduate Research Fellowship.

■ REFERENCES

- (1) Boyen, H.-G.; Ziemann, P.; Wiedwald, U.; Ivanova, V.; Kolb, D. M.; Sakong, S.; Gross, A.; Romanyuk, A.; Buttner, M.; Oelhafen, P. Local density of states effects at the metal-molecule interfaces in a molecular device. *Nat. Mater.* **2006**, *5*, 394–399.
- (2) Koch, N. Organic electronic devices and their functional interfaces. *ChemPhysChem* **2007**, *8*, 1438–1455.
- (3) Duhm, S.; Heimel, G.; Salzmann, I.; Glowatzki, H.; Johnson, R. L.; Vollmer, A.; Rabe, J. P.; Koch, N. Orientation-dependent ionization energies and interface dipoles in ordered molecular assemblies. *Nat. Mater.* **2008**, *7*, 326–332.
- (4) Tseng, T.-C.; Urban, C.; Wang, Y.; Otero, R.; Tait, S. L.; Alcamí, M.; Écija, D.; Trelka, M.; Gallego, J. M.; Lin, N.; Konuma, M.; Starke, U.; Nefedov, A.; Langner, A.; Wöll, C.; Herranz, M. Á.; Martín, F.; Martín, N.; Kern, K.; Miranda, R. Charge-transfer-induced structural rearrangements at both sides of organic/metal interfaces. *Nat. Chem.* **2010**, *2*, 374–379.
- (5) Vitali, L.; Levita, G.; Ohmann, R.; Comisso, A.; De Vita, A.; Kern, K. Portrait of the potential barrier at metal-organic nanocontacts. *Nat. Mater.* **2010**, *9*, 320–323.
- (6) Hwang, J.; Wan, A.; Kahn, A. Energetics of metal-organic interfaces: New experiments and assessment of the field. *Mater. Sci. Eng. R: Rep.* **2009**, *64*, 1–31.
- (7) Braun, S.; Salaneck, W. R.; Fahlman, M. Energy-Level Alignment at Organic/Metal and Organic/Organic Interfaces. *Adv. Mater.* **2009**, *21*, 1450–1472.
- (8) Witte, G.; Lukas, S.; Bagus, P. S.; Wöll, C. Vacuum level alignment at organic/metal junctions: “Cushion” effect and the interface dipole. *Appl. Phys. Lett.* **2005**, *87*, 263502.
- (9) Huang, P.; Carter, E. A. Self-consistent embedding theory for locally correlated configuration interaction wave functions in condensed matter. *J. Chem. Phys.* **2006**, *125*, 084102.
- (10) Bagus, P. S.; Staemmler, V.; Wöll, C. Exchangelike Effects for Closed-Shell Adsorbates: Interface Dipole and Work Function. *Phys. Rev. Lett.* **2002**, *89*, 096104.
- (11) Neaton, J. B.; Hybertsen, M. S.; Louie, S. G. Renormalization of Molecular Electronic Levels at Metal-Molecule Interfaces. *Phys. Rev. Lett.* **2006**, *97*, 216405.
- (12) Hu, Q.-M.; Reuter, K.; Scheffler, M. Towards an Exact Treatment of Exchange and Correlation in Materials: Application to the “CO Adsorption Puzzle” and Other Systems. *Phys. Rev. Lett.* **2007**, *98*, 176103.
- (13) Sony, P.; Puschnig, P.; Nabok, D.; Ambrosch-Draxl, C. Importance of Van Der Waals Interaction for Organic Molecule-Metal Junctions: Adsorption of Thiophene on Cu(110) as a Prototype. *Phys. Rev. Lett.* **2007**, *99*, 176401.
- (14) Rohlfing, M.; Bredow, T. Binding Energy of Adsorbates on a Noble-Metal Surface: Exchange and Correlation Effects. *Phys. Rev. Lett.* **2008**, *101*, 266106.
- (15) Flores, F.; Ortega, J.; Vázquez, H. Modelling energy level alignment at organic interfaces and density functional theory. *Phys. Chem. Chem. Phys.* **2009**, *11*, 8658.
- (16) Piacenza, M.; D’Agostino, S.; Fabiano, E.; Della Sala, F. Ab initio depolarization in self-assembled molecular monolayers: Beyond conventional density-functional theory. *Phys. Rev. B* **2009**, *80*, 153101.
- (17) Fabiano, E.; Piacenza, M.; D’Agostino, S.; Della Sala, F. Towards an accurate description of the electronic properties of the biphenylthiol/gold interface: The role of exact exchange. *J. Chem. Phys.* **2009**, *131*, 234101.
- (18) Schimka, L.; Harl, J.; Stroppa, A.; Grüneis, A.; Marsman, M.; Mittendorfer, F.; Kresse, G. Accurate surface and adsorption energies from many-body perturbation theory. *Nat. Mater.* **2010**, *9*, 741–744.
- (19) Heimel, G.; Romaner, L.; Brédas, J.-L.; Zoyer, E. Interface Energetics and Level Alignment at Covalent Metal-Molecule Junctions: pi-Conjugated Thiols on Gold. *Phys. Rev. Lett.* **2006**, *96*, 196806.
- (20) Heimel, G.; Romaner, L.; Zoyer, E.; Bredas, J. L. Toward Control of the Metal–Organic Interfacial Electronic Structure in Molecular Electronics: A First-Principles Study on Self-Assembled

- Monolayers of π -Conjugated Molecules on Noble Metals. *Nano Lett.* **2007**, *7*, 932–940.
- (21) Romaner, L.; Heimel, G.; Brédas, J.-L.; Gerlach, A.; Schreiber, F.; Johnson, R. L.; Zegenhagen, J.; Duhm, S.; Koch, N.; Zojer, E. Impact of Bidirectional Charge Transfer and Molecular Distortions on the Electronic Structure of a Metal-Organic Interface. *Phys. Rev. Lett.* **2007**, *99*, 256801.
 - (22) Rusu, P. C.; Brocks, G. Work functions of self-assembled monolayers on metal surfaces by first-principles calculations. *Phys. Rev. B* **2006**, *74*, 073414.
 - (23) Monti, O. L. A.; Steele, M. P. Influence of Electrostatic Fields on Molecular Electronic Structure: Insights for Interfacial Charge Transfer. *Phys. Chem. Chem. Phys.* **2010**, *12*, 12390–12400.
 - (24) Mott, N. F.; Littleton, M. J. Conduction in Polar Crystals. I. Electrolytic Conduction in Solid Salts. *Trans. Faraday Soc.* **1938**, *34*, 485–499.
 - (25) Rissner, F.; Egger, D. A.; Romaner, L.; Heimel, G.; Zojer, E. The Electronic Structure of Mixed Self-Assembled Monolayers. *ACS Nano* **2010**, *4*, 6735–6746.
 - (26) Natan, A.; Kronik, L.; Haick, H.; Tung, R. T. Electrostatic Properties of Ideal and Non-ideal Polar Organic Monolayers: Implications for Electronic Devices. *Adv. Mater.* **2007**, *19*, 4103–4117.
 - (27) Alloway, D. M.; Graham, A. L.; Yang, X.; Mudalige, A.; Colorado, R.; Wysocki, V. H.; Pemberton, J. E.; Randall Lee, T.; Wysocki, R. J.; Armstrong, N. R. Tuning the Effective Work Function of Gold and Silver Using ω -Functionalized Alkanethiols: Varying Surface Composition through Dilution and Choice of Terminal Groups. *J. Phys. Chem. C* **2009**, *113*, 20328–20334.
 - (28) Blumenfeld, M. L.; Steele, M. P.; Ilyas, N.; Monti, O. L. A. Interfacial Electronic Structure of Vanadyl Naphthalocyanine on Highly Oriented Pyrolytic Graphite. *Surf. Sci.* **2010**, *604*, 1649–1657.
 - (29) Blumenfeld, M. L.; Steele, M. P.; Monti, O. L. A. Near- and Far-Field Effects on Molecular Energy Level Alignment at an Organic/Electrode Interface. *J. Phys. Chem. Lett.* **2010**, *1*, 145–148.
 - (30) Fukagawa, H.; Yamane, H.; Kera, S.; Okudaira, K. K.; Ueno, N. Experimental Estimation of the Electric Dipole Moment and Polarizability of Titanyl Phthalocyanine Using Ultraviolet Photoelectron Spectroscopy. *Phys. Rev. B* **2006**, *73*, 041302.
 - (31) Fukagawa, H.; Hosoumi, S.; Yamane, H.; Kera, S.; Ueno, N. Dielectric properties of polar-phthalocyanine monolayer systems with repulsive dipole interaction. *Phys. Rev. B* **2011**, *83*, 085304.
 - (32) Steele, M. P.; Blumenfeld, M. L.; Monti, O. L. A. Experimental Determination of the Excited State Polarizability and Dipole Moment in a Thin Organic Semiconductor Film. *J. Phys. Chem. Lett.* **2010**, *1*, 2011–2016.
 - (33) Steele, M. P.; Blumenfeld, M. L.; Monti, O. L. A. Image States at the Interface of a Dipolar Organic Semiconductor. *J. Chem. Phys.* **2010**, *133*, 124701.
 - (34) Stadler, C.; Hansen, S.; Kröger, I.; Kumpf, C.; Umbach, E. Tuning Intermolecular Interaction in Long-Range-Ordered Submonolayer Organic Films. *Nat. Phys.* **2009**, *5*, 153–158.
 - (35) Stadler, C.; Hansen, S.; Pollinger, F.; Kumpf, C.; Umbach, E.; Lee, T.-L.; Zegenhagen, J. Structural investigation of the adsorption of SnPc on Ag(111) using normal-incidence x-ray standing waves. *Phys. Rev. B* **2006**, *74*, 035404.
 - (36) Baran, J. D.; Larsson, J. A.; Woolley, R. A. J.; Cong, Y.; Moriarty, P. J.; Cafolla, A. A.; Schulte, K.; Dhanak, V. R. Theoretical and experimental comparison of SnPc, PbPc, and CoPc adsorption on Ag(111). *Phys. Rev. B* **2010**, *81*, 075413.
 - (37) Yamane, H.; Gerlach, A.; Duhm, S.; Tanaka, Y.; Hosokai, T.; Mi, Y. Y.; Zegenhagen, J.; Koch, N.; Seki, K.; Schreiber, F. Site-Specific Geometric and Electronic Relaxations at Organic-Metal Interfaces. *Phys. Rev. Lett.* **2010**, *105*, 046103.
 - (38) Heinrich, B. W.; Iacovita, C.; Brumme, T.; Choi, D.-J.; Limot, L.; Rastei, M. V.; Hofer, W. A.; Kortus, J.; Bucher, J.-P. Direct Observation of the Tunneling Channels of a Chemisorbed Molecule. *J. Phys. Chem. Lett.* **2010**, *1*, 1517–1523.
 - (39) Gerlach, A.; Hosokai, T.; Duhm, S.; Kera, S.; Hofmann, O. T.; Zojer, E.; Zegenhagen, J.; Schreiber, F. Orientational Ordering of Nonplanar Phthalocyanines on Cu(111): Strength and Orientation of the Electric Dipole Moment. *Phys. Rev. Lett.* **2011**, *106*, 156102.
 - (40) Stadtmüller, B.; Kröger, I.; Reinert, F.; Kumpf, C. Submonolayer growth of CuPc on noble metal surfaces. *Phys. Rev. B* **2011**, *83*, 085416.
 - (41) Cheng, Z. H.; Gao, L.; Deng, Z. T.; Jiang, N.; Liu, Q.; Shi, D. X.; Du, S. X.; Guo, H. M.; Gao, H.-J. Adsorption Behavior of Iron Phthalocyanine on Au(111) Surface at Submonolayer Coverage. *J. Phys. Chem. C* **2007**, *111*, 9240–9244.
 - (42) Gao, L.; Ji, W.; Hu, Y. B.; Cheng, Z. H.; Deng, Z. T.; Liu, Q.; Jiang, N.; Lin, X.; Guo, W.; Du, S. X.; Hofer, W. A.; Xie, X. C.; Gao, H.-J. Site-Specific Kondo Effect at Ambient Temperatures in Iron-Based Molecules. *Phys. Rev. Lett.* **2007**, *99*, 106402.
 - (43) Casarin, M.; Marino, M. D.; Forrer, D.; Sambi, M.; Sedona, F.; Tondello, E.; Vittadini, A.; Barone, V.; Pavone, M. Coverage-Dependent Architectures of Iron Phthalocyanine on Ag(110): a Comprehensive STM/DFT Study. *J. Phys. Chem. C* **2010**, *114*, 2144–2153.
 - (44) Javaid, S.; Bowen, M.; Boukari, S.; Joly, L.; Beaufrand, J.-B.; Chen, X.; Dappe, Y. J.; Scheurer, F.; Kappler, J.-P.; Arabski, J.; Wulfhekel, W.; Alouani, M.; Beaurepaire, E. Impact on Interface Spin Polarization of Molecular Bonding to Metallic Surfaces. *Phys. Rev. Lett.* **2010**, *105*, 077201.
 - (45) Hu, Z.; Li, B.; Zhao, A.; Yang, J.; Hou, J. G. Electronic and Magnetic Properties of Metal Phthalocyanines on Au(111) Surface: A First-Principles Study. *J. Phys. Chem. C* **2008**, *112*, 13650–13655.
 - (46) Paniago, R.; Matzdorf, R.; Goldmann, A. Localization of d-like Surface Resonances on Reconstructed Au(111). *Europhys. Lett.* **1994**, *26*, 63–67.
 - (47) Nicolay, G.; Reinert, F.; Hüfner, S.; Blaha, P. Spin-orbit splitting of the L-gap surface state on Au(111) and Ag(111). *Phys. Rev. B* **2001**, *65*, 033407.
 - (48) TURBOMOLE V6.2 2010, a development of University of Karlsruhe and Forschungszentrum Karlsruhe GmbH 1989–2007; TURBOMOLE GmbH, 2007.
 - (49) Perdew, J. P.; Burke, K.; Ernzerhof, M. Generalized Gradient Approximation Made Simple. *Phys. Rev. Lett.* **1996**, *77*, 3865.
 - (50) All basis sets can be downloaded from bases.turbo-forum.com/TBL/tbl.html (accessed March 4, 2007).
 - (51) Rapoport, D.; Furche, F. Property-optimized Gaussian basis sets for molecular response calculations. *J. Chem. Phys.* **2010**, *133*, 134105.
 - (52) Hoshi, H.; Yamada, T.; Ishikawa, K.; Takezoe, H.; Fukuda, A. Electric quadrupole second-harmonic generation spectra in epitaxial vanadyl and titanyl phthalocyanine films grown by molecular-beam epitaxy. *J. Chem. Phys.* **1997**, *107*, 1687.
 - (53) Zhang, Y.; Learmonth, T.; Wang, S.; Matsuura, A. Y.; Downes, J.; Plucinski, L.; Bernardis, S.; O'Donnell, C.; Smith, K. E. Electronic structure of the organic semiconductor vanadyl phthalocyanine (VO-Pc). *J. Mater. Chem.* **2007**, *17*, 1276.
 - (54) Westcott, B. L.; Gruhn, N. E.; Michelsen, L. J.; Dennis, L. Lichtenberger Experimental Observation of Non-Aufbau Behavior: Photoelectron Spectra of Vanadylctaethylporphyrinate and Vanadylphthalocyanine. *J. Am. Chem. Soc.* **2000**, *122*, 8083.
 - (55) Rosa, A.; Baerends, E. J. Metal-Macrocyclic Interaction in Phthalocyanines: Density Functional Calculations of Ground and Excited States. *Inorg. Chem.* **1994**, *33*, 584.
 - (56) Liao, M.-S.; Scheiner, S. Electronic structure and bonding in metal phthalocyanines, Metal=Fe, Co, Ni, Cu, Zn, Mg. *J. Chem. Phys.* **2001**, *114*, 9780.
 - (57) Lozzi, L.; La Rosa, S.; Delley, B.; Picozzi, S. Electronic structure of crystalline copper phthalocyanine. *J. Chem. Phys.* **2004**, *121*, 1883.
 - (58) Calzolari, A.; Ferretti, A.; Nardelli, M. B. Ab initio correlation effects on the electronic and transport properties of metal(II)-phthalocyanine-based devices. *Nanotechnology* **2007**, *18*, 424013.
 - (59) Marom, N.; Hod, O.; Scuseria, G. E.; Kronik, L. Electronic structure of copper phthalocyanine: A comparative density functional theory study. *J. Chem. Phys.* **2008**, *128*, 164107.
 - (60) Evangelista, F.; Caravetta, V.; Stefan, G.; Jansik, B.; Alagia, M.; Stranges, S.; Ruocco, A. Electronic structure of copper phthalocyanine: An experimental and theoretical study of occupied and unoccupied levels. *J. Chem. Phys.* **2007**, *126*, 124709.

- (61) Giovannetti, G.; Brocks, G.; van den Brink, J. Ab initio electronic structure and correlations in pristine and potassium-doped molecular crystals of copper phthalocyanine. *Phys. Rev. B* **2008**, *77*, 035133.
- (62) Giannozzi, P.; Baroni, S.; Bonini, N.; Calandra, M.; Car, R.; Cavazzoni, C.; Ceresoli, D.; Chiarotti, G. L.; Cococcioni, M.; Dabo, I.; Dal Corso, A.; de Gironcoli, S.; Fabris, S.; Fratesi, G.; Gebauer, R.; Gerstmann, U.; Gouguassis, C.; Kokalj, A.; Lazzeri, M.; Martin-Samos, L.; Marzari, N.; Mauri, F.; Mazzarello, R.; Paolini, S.; Pasquarello, A.; Paulatto, L.; Sbraccia, C.; Scandolo, S.; Sclauzero, G.; Seitsonen, A. P.; Smogunov, A.; Umari, P.; Wentzcovitch, R. M. QUANTUM ESPRESSO: a modular and open-source software project for quantum simulations of materials. *J. Phys.: Condens. Matter* **2009**, *21*, 395502.
- (63) Avdeev, V. I.; Tapilin, V. M. Water Effect on the Electronic Structure of Active Sites of Supported Vanadium Oxide Catalyst VO_x/TiO₂(001). *J. Phys. Chem. C* **2010**, *114*, 3609–3613.
- (64) Petrik, M. V.; Medvedeva, N. I.; Kadyrova, N. I.; Zainulin, Y. G.; Ivanovskii, A. L. Effect of electron correlations on the electronic structure and magnetic properties of the perovskite-like high-pressure phase ErCu₃V₄O₁₂. *Phys. Solid State* **2010**, *52*, 1709–1713.
- (65) Bengtsson, L. Dipole correction for surface supercell calculations. *Phys. Rev. B* **1999**, *59*, 12301.
- (66) Maeland, A.; Flanagan, T. Lattice Spacings of Gold-Palladium Alloys. *Can. J. Phys.* **1964**, *42*, 2364–2366.
- (67) Rusu, P. C.; Giovannetti, G.; Weijtens, C.; Coehoorn, R.; Brocks, G. Work Function Pinning at Metal–Organic Interfaces. *J. Phys. Chem. C* **2009**, *113*, 9974–9977.
- (68) Romaner, L.; Nabok, D.; Puschnig, P.; Zojer, E.; Ambrosch-Draxl, C. Theoretical study of PTCDA adsorbed on the coinage metal surfaces, Ag(111), Au(111) and Cu(111). *New J. Phys.* **2009**, *11*, 053010.
- (69) Duhm, S.; Gerlach, A.; Salzmann, I.; Bröker, B.; Johnson, R. L.; Schreiber, F.; Koch, N. PTCDA on Au(111), Ag(111) and Cu(111): Correlation of interface charge transfer to bonding distance. *Org. Electron.* **2008**, *9*, 111–118.
- (70) Toyoda, K.; Hamada, I.; Lee, K.; Yanagisawa, S.; Morikawa, Y. Density functional theoretical study of pentacene/noble metal interfaces with van der Waals corrections: Vacuum level shifts and electronic structures. *J. Chem. Phys.* **2010**, *132*, 134703.
- (71) Henze, S. K. M.; Bauer, O.; Lee, T.-L.; Sokolowski, M.; Tautz, F. S. Vertical bonding distances of PTCDA on Au(111) and Ag(111): Relation to the bonding type. *Surf. Sci.* **2007**, *601*, 1566–1573.
- (72) Rusu, P. C.; Giovannetti, G.; Weijtens, C.; Coehoorn, R.; Brocks, G. First-principles study of the dipole layer formation at metal–organic interfaces. *Phys. Rev. B* **2010**, *81*, 125403.
- (73) Tkatchenko, A.; Romaner, L.; Hofmann, O.; Zojer, E.; Ambrosch-Draxl, C.; Scheffler, M. Van der Waals Interactions Between Organic Adsorbates and at Organic/Inorganic Interfaces. *MRS Bull.* **2010**, *35*, 435–442.
- (74) McNellis, E. R.; Meyer, J.; Reuter, K. Azobenzene at coinage metal surfaces: Role of dispersive van der Waals interactions. *Phys. Rev. B* **2009**, *80*, 205414.
- (75) Lee, K.; Yu, J.; Morikawa, Y. Comparison of localized basis and plane-wave basis for density-functional calculations of organic molecules on metals. *Phys. Rev. B* **2007**, *75*, 045402.
- (76) Tonigold, K.; Groß, A. Adsorption of small aromatic molecules on the (111) surfaces of noble metals: A density functional theory study with semiempirical corrections for dispersion effects. *J. Chem. Phys.* **2010**, *132*, 224701.
- (77) Grimme, S. Semiempirical GGA-type density functional constructed with a long-range dispersion correction. *J. Comput. Chem.* **2006**, *27*, 1787–1799.
- (78) Barone, V.; Casarin, M.; Forrer, D.; Pavone, M.; Sambi, M.; Vittadini, A. Role and effective treatment of dispersive forces in materials: Polyethylene and graphite crystals as test cases. *J. Comput. Chem.* **2009**, *30*, 934–939.
- (79) Fabiano, E.; Constantin, L. A.; Della Sala, F. Exchange-correlation generalized gradient approximation for gold nanostructures. *J. Chem. Phys.* **2011**, *134*, 194112.
- (80) Nguyen, M.-T.; Pignedoli, C. A.; Treier, M.; Fasel, R.; Passerone, D. The role of van der Waals interactions in surface-supported supramolecular networks. *Phys. Chem. Chem. Phys.* **2010**, *12*, 992.
- (81) Duncan, D. A.; Unterberger, W.; Hogan, K. A.; Lerotholi, T. J.; Lamont, C. L. A.; Woodruff, D. P. A photoelectron diffraction investigation of vanadyl phthalocyanine on Au(111). *Surf. Sci.* **2010**, *604*, 47–53.
- (82) Topping, J. On the Mutual Potential Energy of a Plane Network of Doublets. *Proc. R. Soc. London A* **1927**, *114*, 67–72.
- (83) Hasegawa, S.; Tanaka, S.; Yamashita, Y.; Inokuchi, H.; Fujimoto, H.; Kamiya, K.; Seki, K.; Ueno, N. Molecular orientation in thin films of bis(1,2,5-thiadiazolo)-p-quinonobis(1,3-dithiole) on graphite studied by angle-resolved photoelectron spectroscopy. *Phys. Rev. B* **1993**, *48*, 2596.
- (84) Barlow, D. E.; Hipp, K. W. A Scanning Tunneling Microscopy and Spectroscopy Study of Vanadyl Phthalocyanine on Au(111): the Effect of Oxygen Binding and Orbital Mediated Tunneling on the Apparent Corrugation. *J. Phys. Chem. B* **2000**, *104*, 5993–6000.
- (85) Chizhov, I.; Scoles, G.; Kahn, A. The influence of steps on the orientation of copper phthalocyanine monolayers on Au(111). *Langmuir* **2000**, *16*, 4358–4361.
- (86) Zhang, Y.-F.; Isshiki, H.; Katoh, K.; Yoshida, Y.; Yamashita, M.; Miyasaka, H.; Breedlove, B. K.; Kajiwara, T.; Takaishi, S.; Komeda, T. A Low-Temperature Scanning Tunneling Microscope Investigation of a Nonplanar Dysprosium–Phthalocyanine Adsorption on Au(111). *J. Phys. Chem. C* **2009**, *113*, 14407–14410.
- (87) Cheng, Z. H.; Gao, L.; Deng, Z. T.; Jiang, N.; Liu, Q.; Shi, D. X.; Du, S. X.; Guo, H. M.; Gao, H.-J. Adsorption Behavior of Iron Phthalocyanine on Au(111) Surface at Submonolayer Coverage. *J. Phys. Chem. C* **2007**, *111*, 9240–9244.
- (88) Ziroff, J.; Gold, P.; Bendounan, A.; Forster, F.; Reinert, F. Adsorption Energy and Geometry of Physisorbed Organic Molecules on Au(111) Probed by Surface-State Photoemission. *Surf. Sci.* **2009**, *603*, 354–358.
- (89) Forrest, S. R.; Zhang, Y. Ultrahigh-vacuum quasiepitaxial growth of model van der Waals thin films. I. Theory. *Phys. Rev. B* **1994**, *49*, 11297.
- (90) Xiao, J.; Dowben, P. A. Changes in the adsorbate dipole layer with changing d-filling of the metal (II) (Co, Ni, Cu) phthalocyanines on Au(111). *J. Phys.: Condens. Matter* **2009**, *21*, 052001.